PIV measurements of a Wake from a Rough Flat Plate

S. Lawrence, C. Atkinson, J. Soria

Laboratory for Turbulence Research in Aerospace and Combustion,
Department of Mechanical and Aerospace Engineering, Monash University, Melbourne 3800, Australia

Abstract

The structure of the wake behind a submersed body greatly affects the performance and design of many engineering applications. The behaviour of the wake partially dictates the drag experienced by the body, therefore optimisation of this wake behaviour can have a significant effect on the energy required to move the body relative to the fluid. The formation of wakes over smooth bodies is well understood, however, the implications of surface roughness on the near wake structure are not well known. Surface roughness is known to greatly affect the behaviour of a turbulent boundary layer and the nature of the structures within. The subsequent interaction of these modified boundary layers in the wake modifies the formation of the wake. Roughness can be introduced into a system in a range of ways, such as manufacturing processes, surface finishes and degradation and accumulation of fouling. Therefore, the prevalence of roughness in combination with the importance of wake behaviour on performance is the motivation for the investigation of the implications of surface roughness on plane wake flows.

To investigate these implications a series of 2-component - 2-dimensional particle image velocimetry (2C-2D PIV) measurements were performed on a smooth and rough flat plate in the LTRAC large horizontal water tunnel facility. The boundary layer was tripped at the leading edge and measurements were acquired in the near wake of the blunt trailing edge of the plate. The surface was roughened using commercially available sandpaper adhered to the plate surface.

Introduction

Wake flows are prevalent in a range of engineering application and have a significant impact on performance and design. The drag experienced by engineering components such as aerofoils, turbine blades and submersed vehicles is significantly impacted by the behaviour of the wake. The structure and behaviour of a wake formed by uniform flow over a smooth body is well understood, however there has been little investigation into the effect of surface roughness on the wake.

Surface roughness can be introduced into a system in a range of ways. Material type, manufacturing methods and surface finishes are all factors that can introduce roughness into a system. In addition to this, surface degradation and the build up of fouling over time can further contribute to the roughness. The consequences of increased surface roughness can be severe. Fouling buildup has been estimated to increase frictional resistance by up to 217% on a mid sized merchant ship or Naval frigate or destroyer, depending on the surface coating used [8]. This highlights the extent to which surface roughness can effect the efficiency of engineering systems.

At present a reasonable understand of the effect of surface roughness has been developed. A surface is only seen as rough by the flow if the roughness elements extend out past the viscous sublayer, otherwise it is considered to be hydraulically smooth [7]. Once the roughness extends past the viscous sublayer it begins to impact the behaviour of the buffer layer viscous cycle. If its size is not negligible with respect to the boundary layer

thickness then it can affect the whole flow. Surface roughness can affect the mean flow by modifying the friction coefficient and shifting the effective origin of the boundary layer such that the rough wall mean profile is offset from the smooth wall mean profile by the roughness function, ΔU^+ [4].

In the case of a wake behind a flat plate, the boundary layer develops over the length of the body and forms the initial conditions for the wake. Experimental results suggest that the wake remembers the shape of the body that it forms behind. Spread rates have been found to differ depending on the generator, such as a plate, cylinder or airfoil [6]. Therefore it is reasonable to assume that modifications to the boundary layer resulting from surface roughness would also impact the wake development as they are analogous to a difference generator for the wake.

By affecting the initial conditions surface roughness impacts both aspects of drag; form drag and skin friction. A significant body of work exists on the impacts of surface roughness on the boundary layer and skin friction [4], often with an emphasis on marine fouling [5, 8, 9]. The same cannot be said for form drag. Some work exists on the effect of surface roughness on wakes in a flow control capacity [1]. However, a detailed catalogue of experiments and understanding of the effect of surface roughness on wake flows is lacking.

The wake of a smooth flat plate forms a two-dimensional, statistically stationary flow which is symmetric about the span-wise plane. In the case of a wake created by a blunt trailing edge, the flow will exhibit a re-circulation region caused by flow separation at the trailing edge. A shear layer will consequently form between this low velocity region and the faster moving outer flow on each side of the wake. The behaviour of the shear layer will be largely characterised by the preceding boundary layer formed along the plate.

As per Pope [6] a characteristic velocity difference relative to the free-stream convective velocity, U_c, can be defined as

$$U_s(x) = U_c - \overline{U}(x,0,0) \qquad (1)$$

and the half-width of the wake, $y_{1/2}$ as

$$\overline{U}(x, \pm y_{1/2}, 0) = U_c - \frac{1}{2}U_s(x). \qquad (2)$$

The wake can be separated into two primary regions, the near wake and the far wake. The far wake exhibits asymptotically self-similar behaviour as the flow forgets the specific obstacle shape that it originated from. Experiments indicate that the self-similar region occurs when the ratio of U_s/U_c is below $\frac{1}{10}$ [6]. The near wake is somewhat more complex as there is a greater dependence on the initial conditions of the wake provided by the plate and self-similarity is not present. In this region the boundary layers from each side of the plate merge and flow interacts with the plate. The mean profile of a wake flow depends on the stream-wise distance from the trailing edge of the plate. As the wake convects downstream the wake will spread and the velocity difference will tend towards zero. The half width, $y_{1/2}$,
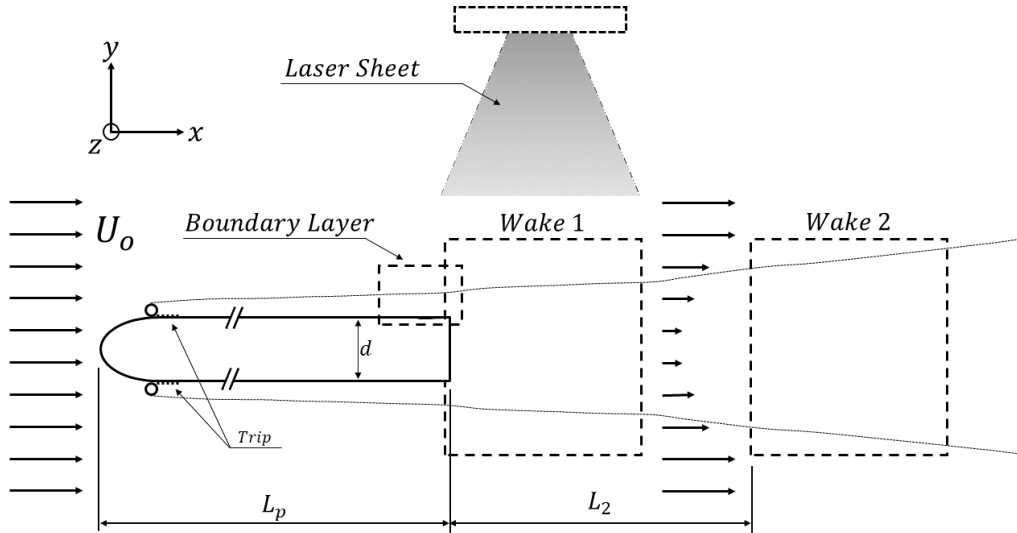
Figure 1: Diagram of the experimental setup and regions of interest.

and the centre-line velocity difference, U_s, vary with $x^{1/2}$ and $x^{-1/2}$, respectively [6].

The purpose of the initial exploratory experiment presented here is to identify what differences exist between the wakes behind smooth and rough flat plates. This will form the basis for what aspects of the flow need to be investigated further to provide a complete characterisation of the effect of surface roughness on wake flows.
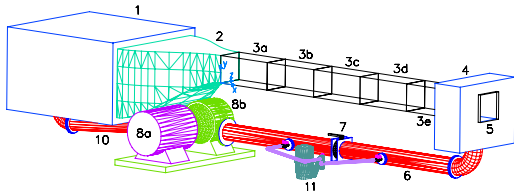
Experiment

Figure 2: Diagram of the LTRAC large horizontal water tunnel facility; 1) Settling chamber, 2) 10:1 contraction, 3) Working sections, 4) Plenum chamber, 5) Rear observation window, 6) Return pipe, 7) Filtration isolation valve, 8) A.C. motor and centrifugal pump system, 10) Return pipework, 11) Water filter.

The experiment was conducting in the LTRAC large horizontal water tunnel facility, figure 2. It is a closed circuit tunnel with five 1m long acrylic working sections, each having a 500 × 500 cross sectional working area. The flow is introduced to the setting chamber through a large perforated PVC pipe spanning the width of the chamber so as to evenly distribute the flow. It then passes through a series of increasingly finer mesh screens and a honey comb, situated between the first and second mesh screens, in order to reduce the background turbulence levels and straighten the flow. The relative turbulence scales are reduced further and the flow accelerated by a 10:1 contraction leading into the working section. Flow return in the plenum chamber is achieved by passing the flow through vertical perforated steel plates which are parallel to the working section walls. This ensures minimal disturbance of the upstream flow while redirecting the flow through a 300 mm return pipe to the in-line

centrifugal pump system run by a 53 kW a.c. motor. The tunnel is capable of producing a maximum flow speed of 775 mm/s.

Data was collected in the fourth working section at a location 3500mm from the end of the contraction (3d in figure 2). An acrylic plate measuring 610mm long, 500mm wide and 19.2mm thick was placed vertically in tunnel upstream of the data collection station. A diagram of the plate and the regions of interest are shown in figure 1. The plate had a 45mm long semi-elliptical leading edge and a blunt trailing edge. The flow was tripped at the end of the leading edge where the plate thickness becomes constant using a 5mm diameter steel rod and a 55mm wide strip of P80 sandpaper spanning the full width of the plate. The development length of the flow from the end of the trip to the trailing edge of the plate was 510 mm. Measurements were taken for a smooth base case and a single roughness case. The smooth measurements were performed on the smooth acrylic plate and a rough surface was created by adhering P400 'wet or dry' sandpaper over the full development length. The sandpaper has a mean particle diameter of $35.0 \mu m$ (as per ISO 6344) and is silicon carbide abrasive material on a water resistant paper backing. It was adhered to the acrylic using a thin layer of commercially available silicone adhesive suitable for underwater line use.

2C-2D PIV measurements were taken at two locations as indicated in figure 1. The field of view (FOV) for both locations was approximately 203 × 171 mm and centered on the plate. The first location, denoted 'Wake 1' in the diagram, was captured with 2 mm of the plate in the FOV. The plate was centred and aligned in the tunnel so it could be traversed upstream 155 mm using linear rails to capture the second region, denoted as 'Wake 2'. Measurements in the two locations were taken consecutively to ensure minimal variation in the flow conditions. This resulted in data being collected up to 15 plate thickness downstream. Images were obtained using a 5.5MP ILA sC-MOS camera at full sensor size of 2560 × 2160 px and a Zeiss Makro-Planar 2/50 ZF.2 lens mounted below the tunnel. A horizontal region of interest, parallel with the floor, was captured by directing the light 90 degrees using a front coated mirror to the camera, whose sensor was perpendicular to the region of interest. The camera was operated in double shutter mode and the images were saved directly to the hard drive of a computer

connected to the camera at a frequency of $15Hz$.

Seeding was provided by $11\mu m$ diameter Potters hollow glass spheres with specific gravity $\gamma = 1.1$. They were illuminated by a New Wave Nd:YAG pulsed laser capable of producing $120mJ$ pulses at $532nm$ at a repetition rate of $15Hz$. A sheet was created using cylindrical lenses with an approximate thickness of $1.5mm$. Control of the planer DPIV system was provided by an in house timing controller using a BeagleBone Black single-board open source computer with a Programmable Real-Time Unit as described in [2].

The raw images were processed using an in house DPIV code implementing the multi-grid cross-correlation digital particle image velocimetry (MCCDPIV) algorithm described in [11] and originating from [10]. The algorithm increases the velocity dynamic range through the use of an iterative and adaptive cross-correlation algorithm which also reduces the random and bias error. Additionally, a local cross-correction function multiplication method is incorporated in the MCCDPIV algorithm to increase the quality of the cross-correlation peaks found and reduce error, as detailed in [3].

The wake images were analysed using 128×128 px interrogation windows on the first pass and 32×32 px on the second pass. Vectors were calculated on a 16×8 grid. Data validation was performed using a dynamic mean value operator test and a median test [12]. Ensemble average velocity components in the stream-wise and cross-steam directions were extracted and are denoted herein as $\overline{U}$ and $\overline{V}$, respectively.

Magnification	0.08
Spatial resolution (mm/px)	0.08
Lens aperture	$f/2$
Field of view (mm)	202×171
First IW size ($x \times y$ px)	128×128
Second IW size ($x \times y$ px)	32×32
Vector spacing ($x \times y$ px)	16×8

Table 1: Parameters for the PIV setup.

Results

To investigate the behaviour of the wake samples of 1000 images pairs were acquired in each measurement location, and the resulting 1000 vector fields were ensemble averaged to extract mean statistics. For the purpose of the analysis the origin is taken as the centre of the trailing edge, with x representing the stream-wise direction and y representing the cross-stream direction. From the mean stream-wise velocity, $\overline{U}$, the deficit profile was calculated as

$$U_D(x,y) = U_c - \overline{U}(x,y,0), \qquad (3)$$

and used to determine the half width, $y_{1/2}$ and the characteristic velocity difference, U_s. The half width was found by linearly interpolating between the discrete velocity measurements in the profile. A characteristic length of the half width of the plate is used to non-dimensionalise in the stream-wise direction and is denoted by $d_{1/2}$.

The development of the half widths of the wakes for the smooth and rough plate are shown in figure 3 along with a line of best fit following the theoretical variation of $y_{1/2}$ as $x^{1/2}$. The fit was performed on the data between $6.6 < x/d_{1/2} < 29.2$. The half width of the rough wake increases more rapidly than that of the smooth wake until $x/d_{1/2} \approx 6$. After this point the growth rate of the half widths for both cases is similar. The half width for the rough wake remains between 0.19 and 0.14 half plate widths larger than the smooth wake half width in this region. The data
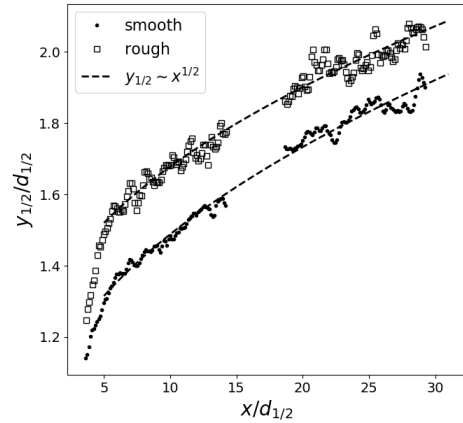

Figure 3: Stream-wise development of the half width, non-dimensionalised by the half plate thickness for the smooth and rough wakes.

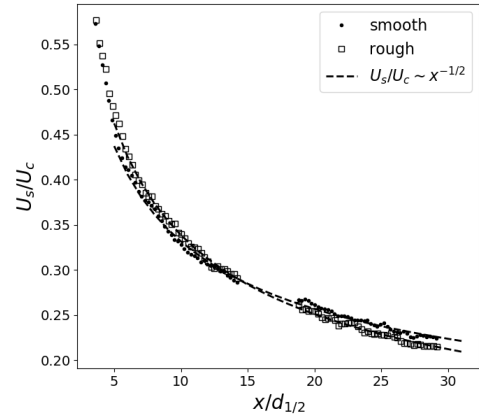for both cases shows reasonable agreement with the theoretical relationship.

Figure 4: Stream-wise development of the centre-line velocity difference, non-dimensionalised by the outer convective velocity for the smooth and rough wakes.

Similar to the half width development, the centre-line velocity difference should decay proportional to $x^{-1/2}$. To compare the two cases the centre-line velocity difference, U_s, was normalised by the free-steam velocity, U_c, and the ratio is shown in figure 4. The ratio for the two cases is similar until $x/d_{1/2} \approx 5$, past which the smooth wake has a lower value until a cross over point at $x/d_{1/2} \approx 13$. As the flow moves further downstream, the rough wake has a lower centre-line velocity difference, which appears to be decreasing at a slightly faster rate than the smooth case. Self-similar behaviour can be expected once the ratio of U_s/U_c IS below about $\frac{1}{10}$ for experiments [6]. Therefore the data suggests that the rough wake would reach a self-similar state at a distance closer to the plate than the smooth wake.

A contour plot of the mean stream-wise velocity as a percentage of the free-stream velocity is shown in figure 5. The location of the plate is represented by the grey rectangle on the left and flow
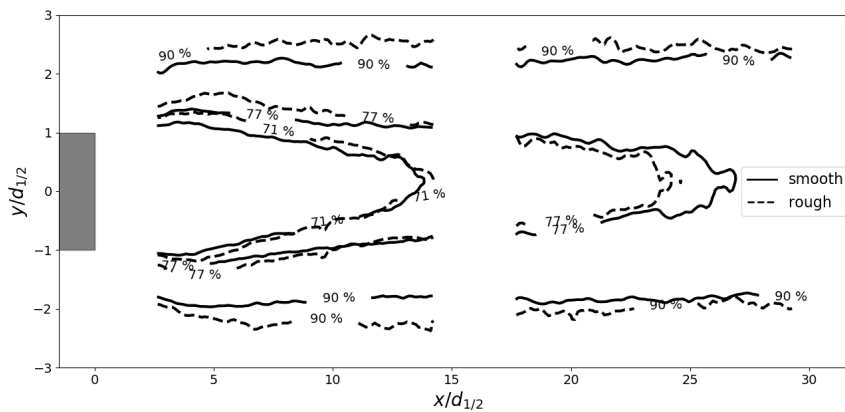
Figure 5: Contour plot of the stream-wise velocity as a percentage of the free-stream velocity for the smooth and rough cases, showing the location of the plate, with the flow moving from left to right.

is moving from left to right. The contours shown here agree with the afore mentioned observations. The 90% contour for the rough wake is wider over the whole domain, indicating that the rough wake is spread wider than the smooth wake. This is consistent with the relationship shown by the half width development. The 71% and 77% lines behave in a consistent manner with regards to the centre-line velocity relationship. The centre-line at the 71% line indicates that the smooth wake is recovering the velocity difference closer to the plate than the rough plate at that location, while the centre-line at the 77% line shows the opposite. This is consistent with the centre-line velocity difference data shown in figure 4.

Conclusions

A series of 2C-2D PIV measurements were performed on the near wakes of a smooth and rough flat plate. The plate was roughened with P400 'wet and dry' sandpaper with a mean particle diameter of 35.0μm and measurements were taken up to 15 plate thicknesses downstream of the plate.

It was observed that the roughness caused the half width of the wake to grow more rapidly near the plate before approximately matching the growth rate of the smooth case. The half width was 0.14 to 0.19 plate half thicknesses greater in the rough case over the observed domain. The center-line velocity difference for the rough wake was initially higher than for the smooth wake. However, for $x/d_{1/2} \gtrsim 13$ the rough difference was lower and decreasing at a slightly higher rate, indicating that it could reach a self-similar state at a shorter downstream distance than in the smooth case. These observations confirmed that the surface roughness does impact the wake development and justifies further investigation.

Acknowledgements

References

[1] Choi, H., Jeon, W.-P. and Kim, J., Control of flow over a bluff body, *Annual Review of Fluid Mechanics*, **40**, 2008, 113–139.

[2] Fedrizzi, M. and Soria, J., Application of a single-board computer as a low-cost pulse generator, *Measurement Science and Technology*, **26**, 2015, 095302.

[3] Hart, D. P., Piv error correction, *Experiments in Fluids*, **29**, 2000, 13–22.

[4] Jiménez, J., Turbulent flows over rough walls, *Annual Review of Fluid Mechanics*, **36**, 2004, 173–196.

[5] Monty, J. P., Dogan, E., Hanson, R., Scardino, A. J., Ganapathisubramani, B. and Hutchins, N., An assessment of the ship drag penalty arising from light calcareous tubeworm fouling, *Biofouling*, **32**, 2016, 451–464.

[6] Pope, S. B., *Turbulent flows*, IOP Publishing, 2001.

[7] Schlichting, H. and Gersten, K., *Boundary-Layer Theory*, Springer Berlin Heidelberg, 2016.

[8] Schultz, M. P., Frictional resistance of antifouling coating systems, *Journal of Fluids Engineering*, **126**, 2005, 1039–1047.

[9] Schultz, M. P. and Flack, K. A., The rough-wall turbulent boundary layer from the hydraulically smooth to the fully rough regime, *Journal of Fluid Mechanics*, **580**, 2007, 381–405.

[10] Soria, J., An investigation of the near wake of a circular cylinder using a video-based digital cross-correlation particle image velocimetry technique, *Experimental Thermal and Fluid Science*, **12**, 1996, 221 – 233.

[11] Soria, J., Cater, J. and Kostas, J., High resolution multigrid cross-correlation digital piv measurements of a turbulent starting jet using half frame image shift film recording, *Optics and Laser Technology*, **31**, 1999, 3 – 12.

[12] Westerweel, J., Efficient detection of spurious vectors in particle image velocimetry data, *Experiments in Fluids*, **16**, 1994, 236–247.